COMPUTATIONAL STUDY OF THE SPECTRAL BROADENING OF AN ACOUSTIC TONE BY TURBULENCE

Vincent Clair *and* Gwénaël Gabard
Institute of Sound and Vibration Research, University of Southampton, UK
email: V.J.Clair@soton.ac.uk

Spectral broadening results from the unsteady scattering of acoustic waves propagating across a region of turbulence. This phenomenon has been observed previously for an harmonic source radiating through the shear layer of a cold jet at low speed. The resulting spectra displayed a reduced tone peak surrounded by lateral bands, with changes in these bands levels and width depending on the source and flow parameters. In this paper, spectral broadening is studied numerically for a simple configuration, consisting of a monopole radiation scattered by a turbulent layer with a constant thickness and convected by a uniform mean velocity. The numerical method relies on a finite difference code solving the linearized Euler equations in the time domain. The turbulent layer is synthesized with a stochastic method based on the filtering of white noise to impose prescribed statistical properties to the turbulence. The turbulent fluctuations are then added to the steady mean flow to form an unsteady base flow around which the Euler equations are linearized. This introduces terms involving products between the turbulent and acoustic fluctuations which are responsible for the scattering. Such a numerical methodology allows to vary the properties of the turbulence generated for the chosen configuration such as the turbulent kinetic energy and the integral length scale. In this paper, the effects of several parameters such as the convection velocity and source frequency on the spectral broadening are studied. The trends deduced from the results can be compared to previous models and experimental data for a jet shear layer, and they can also be related to the trends observed in a previous study of the scattering of sound by a single convected vortex.

1. Introduction

A scattering phenomenon occurs when acoustic waves propagate through a volume of turbulence. The first studies of this phenomenon have been realized by Lighthill [20] and Kraichnan [18] using Lighthill's acoustic analogy and assuming that the scattering is weak (meaning that only a small proportion of the acoustic energy is scattered). The work of Lighthill was focused on the spatial scattering of the acoustic energy, while Kraichnan also expressed the frequency spectrum, particularly for isotropic turbulence. Kinetic equations have been derived by Howe [17], in which the different terms can be linked either to the spatial or spectral scattering. These equations are able to represent multiple scattering whereas the previous models relied on the hypothesis of single scattering across the turbulent volume.

Acoustic scattering by turbulence also received attention in the context of atmospheric propagation. Brown [1] and Brown & Clifford [2, 3] developed a model based on an inhomogeneous

Helmholtz equation with a source term involving the turbulent velocity and temperature fluctuations. Goedecke *et al.* [16] proposed a semi-analytical model based on the scattering by a single eddy. A turbulent volume is split into cells of different sizes containing an eddy, and the scattering by the whole volume is obtained by computing the scattering by each eddy.

The propagation of acoustic radiation through the shear layer of an open wind tunnel or an aero-engine jet is another area of interest for the study of acoustic scattering. These configurations have been studied experimentally by Candel *et al.* [6, 7] and more recently in the framework of the project *GARTEUR AD/AG-50* [19, 23], considering an harmonic source on the jet centerline. The results highlighted a specific shape of the acoustic spectra consisting in an attenuated peak at the source frequency surrounded by sidebands (also called haystacks). Analytical models have also been developed for such configurations, notably by Campos [4, 5], who concluded that widening the shear layer could significantely reduce tonal components propagating through the exhaust of a jet engine, Powles *et al.* [22] and McAlpine *et al.* [21] developed a model to predict the haystacking of turbine tones by either frozen or evolving turbulence. Variations of the source and flow parameters showed behaviours of the acoustic spectra that are consistent with experimental results. The first attempts of numerical calculation of the spectral broadening by a jet shear layer have been performed by Ewert *et al.* [13, 12] and showed promising results in the ability of their method to recover some features of the spectral broadening. Their numerical method relied on the use of the solver *PIANO* and the stochastic method *RPM* to synthesize the turbulent velocity fluctuations of the shear layer.

The work that is presented in this paper uses the same method, to study the scattering of a monopole radiation by an idealized turbulent layer with constant width and convected by a uniform mean flow. This configuration discards the refraction effects by the mean flow and the spreading of the turbulent layer observed for a jet shear layer (leading to an evolution of the scattering along the axis). Moreover, this configuration can be considered as the next step (in terms of complexity) to recent work [8] on the scattering by a single vortex convected by a uniform mean flow. In the present paper, results are presented for several source frequencies and Mach numbers of the unifom mean flow. The shape of the spectra and their evolution displays similarities with previous studies of the spectral broadening by a shear layer, and also strong similarities with the scattering by a single vortex.

2. Numerical method

The *PIANO* solver, developed by the *DLR*, is used in order to solve the linearized Euler equations (*LEE*) in the time domain. This solver has been used in order to study a vast range of problems in acoustics, notably including interactions with turbulence via a coupling with a stochastic turbulence generation method (*RPM* or *fRPM*) [10, 11, 14]. In this paper the RPM is used in order to generate the unsteady velocity fluctuations of the turbulent layer. These fluctuations are generated using an auxiliary grid where random particles are introduced, convected and filtered in space (and eventually time) with a filter defined to enforce prescribed correlations of the velocity. Here the filter ensures Gaussian spatial correlations and no time decorrelation (frozen turbulence). More details on the RPM can be found in [10, 11, 12, 13, 14].

In order to capture the interaction between the incident acoustic field and the convected vortex, the equations have to contain terms involving products between the acoustic fluctuations and the turbulent flow. A set of equations has been developed by Ewert *et al.* [13] by considering small perturbations $(\rho', \boldsymbol{u}', p')$ over an unsteady base flow $(\rho, \boldsymbol{u}, p)$ instead of the usual steady mean flow $(\rho_0, \boldsymbol{u}_0, p_0)$ used in the *LEE*. This unsteady base flow is then split into a steady mean part Ψ_0 and a fluctuating part Ψ^t (here the turbulent velocities): $\Psi(\boldsymbol{x}, t) = \Psi_0(\boldsymbol{x}) + \Psi^t(\boldsymbol{x}, t)$, where Ψ is ρ, $\boldsymbol{u}$ or p.
The equations written using this decomposition are similar to the *LEE*:

$$
\begin{aligned}
&\frac{\partial \rho'}{\partial t} + \boldsymbol{u}_0.\nabla\rho' + \boldsymbol{u}'.\nabla\rho_0 + \rho_0\nabla.\boldsymbol{u}' + \rho'\nabla.\boldsymbol{u}_0 = h_1 \\
&\frac{\partial \boldsymbol{u}'}{\partial t} + (\boldsymbol{u}_0.\nabla)\boldsymbol{u}' + (\boldsymbol{u}'.\nabla)\boldsymbol{u}_0 + \frac{\nabla p'}{\rho_0} - \frac{\nabla p_0 \rho'}{\rho_0^2} = \boldsymbol{h_2} \\
&\frac{\partial p'}{\partial t} + \boldsymbol{u}_0.\nabla p' + \boldsymbol{u}'.\nabla p_0 + \gamma p_0 \nabla.\boldsymbol{u}' + \gamma p'\nabla.\boldsymbol{u}_0 = h_3
\end{aligned} \tag{1}
$$

where all the interaction terms between the acoustic field and the unsteady flow have been moved to the right hand side in $(h_1, \boldsymbol{h_2}, h_3)$. Some assumptions can be made in order to simplify these right hand side terms. First, the unsteady part of the mean flow is assumed to be divergence-free ($\nabla.\boldsymbol{u}^t = 0$), which means that it does not introduce additional sound sources. This hypothesis is ensured when velocity fluctuations are generated with the *RPM*. The second assumption introduced by Ewert *et al.* [13] is that the scattering of the incident acoustic field is mainly induced by the unsteady velocity fluctuations. Thus the effects of the unsteady density and pressure fluctuations are negligible. This assumption has been assessed numerically in [8] for a case of scattering of a plane wave by a steady vortex. Finally, with these simplifications, the right hand side terms of Eq. (1) writes:

$$
\begin{aligned}
h_1 &= -\boldsymbol{u}^t.\nabla\rho' \\
h_2 &= -(\boldsymbol{u}^t.\nabla)\boldsymbol{u}' - (\boldsymbol{u}'.\nabla)\boldsymbol{u}^t \\
h_3 &= -\boldsymbol{u}^t.\nabla p'
\end{aligned} \tag{2}
$$

Ewert *et al.* [13, 12] suffered from growing numerical instabilities when trying to solve these equations, because of the terms of Eq. (1) involving mean flow gradients. In the present paper, since the steady mean flow considered is uniform, therefore there is no gradients and the equations do not require any specific treatment.

The spatial discretization of this set of equations is realized in *PIANO* using the 7 points stencil, 4th order DRP finite differences scheme by Tam & Webb [24], and an explicit 8th order filter is applied in order to prevent high frequency spurious oscillations to appear in the computational domain. The time integration is performed using a 4th order Runge-Kutta time marching scheme with 4 stages. A coordinate transformation is applied in order to deal with curvilinear meshes encountered for complex geometries, and the solver is parallelized using the MPI library. In the computations realized in this paper, the acoustic sources considered are monopoles located relatively far from the vortex path. In order to reduce the computational effort, the monopole radiation is introduced into the numerical domain through a sponge layer located next to a boundary (the lower boundary in this work).

3. Configuration studied

The turbulent layer considered has a constant width δ (centered on the y-axis) and a length 20δ ($-10\delta \leq x \leq 10\delta$). The RPM is used to generate frozen turbulence with Gaussian spatial correlations and an integral length scale $\Lambda = \delta/4$. The turbulent kinetic energy is maximum at $y = 0$ with a turbulent intensity $T_I = 15\%$, and it decreases following a Gaussian progression with $k^t = k^t_{max}/4$ at $y = \pm\delta/2$. The mean flow is uniform, oriented in the $+x$-direction and the the Mach numbers considered are $M = 0.088$, 0.176, 0.352. The acoustic source is an harmonic monopole located at $x = 0$ and $y = -7.5\delta$. The source wavelengths $\lambda_0 = c_0/f_0$ considered in this paper are $\lambda_0 = \delta/2$, δ, 2δ.

A schematic of the numerical domain used for this first calculation is presented in Fig. 1. The grey area represents the auxiliary grid used by the *RPM* to generate the turbulence. The cell spacing on this auxiliary mesh is uniform and ensures $\Lambda \geq 6\Delta x_{RPM}$ as recommended by Dieste & Gabard [9]. The Gaussian filter applied to each random particle in the *RPM* has been shown to receive contributions

from the other particles located at distances $r \leq 2\Lambda$. Thus, to reproduce the correlations correctly over the whole width δ, the auxiliary grid extends up to $y = \pm(\delta/2 + 2\Lambda)$. Random particles are initialized at every nodes of the auxiliary grid and new particles are introduced every $\Delta t_{RPM} = \Delta x_{RPM}/M$.

The computational domains used for the *PIANO* calculations are defined as follows: the domains are uniformly meshed for $-10\delta \leq x \leq 10\delta$ and $-3\delta \leq y \leq 8\delta$ with a cell size ensuring a correct discretization of acoustic waves up to $2f_0$ in every directions. Additional 50 stretched cells sponge layers are defined at the upstream, downstream and upper boundaries to dissipate fluctuations before they reach the boundaries. A sponge layer with uniform cells is also defined at the lower boundary to introduce the monopole radiation in the domain. Tam's radiation and outflow boundary conditions [24] are used with a radiation center defined at the position of the monopole source. A circular array of microphones with a radius $r = 15\delta$, centered on the source position is defined for angles between $50° \leq \theta \leq 130°$ (with $\theta = 0°$ oriented in the $+x$-direction). The timestep of the computations is chosen to ensure a value of the CFL criterion less than 1, and the computations are run over 500,000 iterations to obtain converged statistical properties of the turbulence.

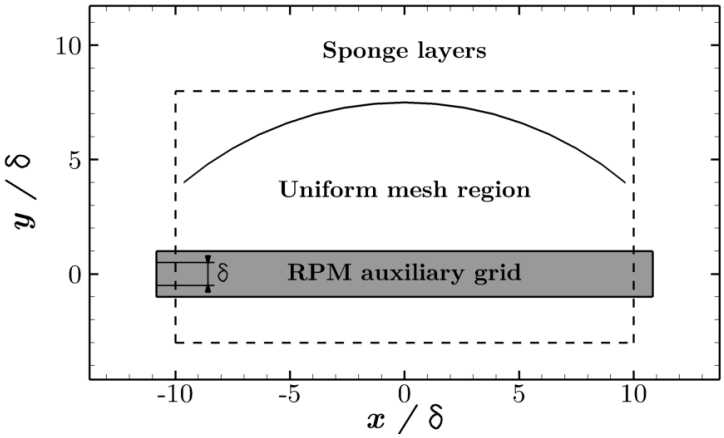

Figure 1: Scheme of the computational domain.

4. Acoustic results

Fig. 2 presents snapshots of the total and scattered pressure fluctuations in the computational domain, as well as contours of the turbulent velocity, for the case $\lambda_0 = \delta$, $M = 0.176$. The alteration of the monopole wavefronts is visible on the total pressure field. The scattered pressure field is obtained by running a similar computation without the turbulent layer, and by subtracting the pressure field without turbulence from the field with turbulence. The scattered field is quite complex (compared to the scattered fields observed in [8] for a single vortex), with interferences between the scattered fields radiated by each turbulent structure/volume. On this snapshot, the turbulent structures located between $-10\delta \leq x \leq 0$ appears to scatter quite efficiently. This spatial distribution of scattered pressure is evolving with time, but the scattered levels in the upstream direction appear to be more important (notably because the incoming radiation from the monopole is more intense upstream due to the convective amplification). For the case presented in Fig. 2, we can also notice that there is very little backscattering (towards the $-y$-direction). The study realized in [8] for a single vortex shows that the backscattering is expected to be more important for low frequency sources.

The pressure time signals recorded on the circular array are used to compute the SPL. The transient period required for the monopole radiation to propagate across the domain at the beginning of the calculation is removed from the signals before performing a periodogram. Fig. 3 presents the spectra calculated from the case $\lambda_0 = \delta$, $M = 0.176$ for different angles. The level of the peak at the incident frequency is normalized by the peak level obtained for a similar calculation without turbulence. The

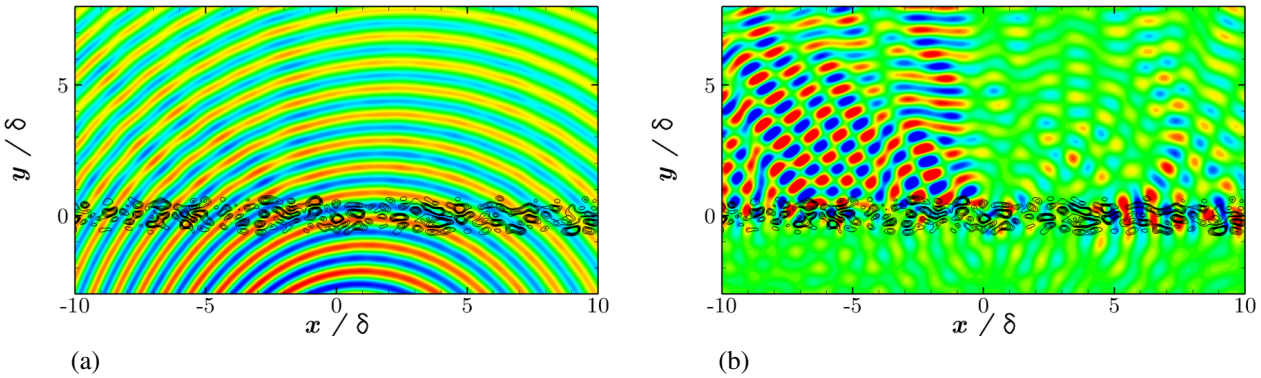

Figure 2: Snapshots of (a) the total pressure fluctuation (levels between $\pm$3.5e-07) and (b) the scattered pressure fluctuation (levels between $\pm$2.5e-08). The lines are the u_t turbulent velocity component (levels between $\pm$0.05).

narrowing of the peak is due to the use of the Hann window in the periodogram. The scattering by the turbulent layer is responsible for the sidebands visible on the spectra. The scattering observed for the configurations studied can be considered to be weak scattering because the reduction of the peak amplitude is nearly invisible here (less than 0.1 dB). These sidebands present similarities with the haystacks that has been observed in previous studies of the scattering by a shear layer and they are also very similar to the side bands observed for the scattering by a single vortex [8]. The width and the levels of the sidebands evolves with the position of the microphone. The higher levels at $\theta = 130°$ (upstream) might partly be due to the convective amplification of the incident monopole. At this angle, the low-frequency sideband is slightly more intense, while the opposite observation can be done for $\theta = 50°$. In addition, we can observe that a secondary lobe is existing at low frequency for $\theta = 130°$ (but not at high frequency) while a secondary lobe only exists at high frequency for $\theta = 50°$. If we consider the turbulent eddies to act as moving sources inducing a Doppler shift, we can relate the position of an eddy to the frequency that will be seen by the microphone. For example, the further upstream a structure is from a microphone, the more the frequency shift (towards the high frequencies) will be important, explaining the appearance of a high frequency secondary lobe at $\theta = 50°$.

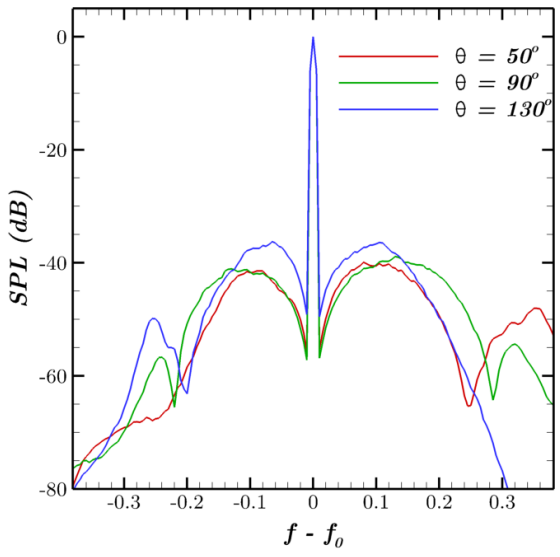

Figure 3: Comparison between the SPL at different microphone positions for the case ($\lambda_0 = \delta$, $M = 0.176$).

Fig. 4(a) presents the results for different frequencies at $\theta = 90°$. The lower frequency case ($\lambda_0 = 2\delta$) is contaminated by instabilities developping when the acoustic waves cross the turbulent layer. These instabilities convect until impacting the downstream boundary and generating intense spurious waves responsible for the low frequency levels on the SPL. Thus, the shape and levels of this spectrum is not really meaningful for $f - f_0 \leq -0.1$. Nevertheless, we can observe an important increase of the scattered levels when the frequency is increased and a change in the width of the sidebands. The sidebands for $\lambda_0 = \delta/2$ are wider than for $\lambda_0 = \delta$ but if we consider them relatively to their respective incident frequency ($(f - f_0)/f_0$), the maxima of the sidebands become closer to the peak for $\lambda_0 = \delta/2$. This can be linked to the results of [8] where it is shown for a single vortex that the main scattering directions of a wave by an eddy get closer to the incident wave propagation direction when the frequency of the source is increased. Thus, the relative Doppler shift becomes less important.

Finally, Fig. 4(b) presents the SPL obtained for different values of the Mach number of the mean flow at $\theta = 90°$. The increase of the scattered levels with Mach number is due to the fact that the turbulent intensity is kept to 15% for the 3 calculations, so the turbulent kinetic energy is increasing with the Mach number. The most visible effect of increasing the Mach number is the widening of the sidebands. It appears that the frequency shifts of the maxima of the sidebands seem to evolve linearly with the Mach number. This relation is in agreement with the hypothesis that the haystacking is linked to a Doppler shift due to the motion of the eddies acting as sources of the scattered field.

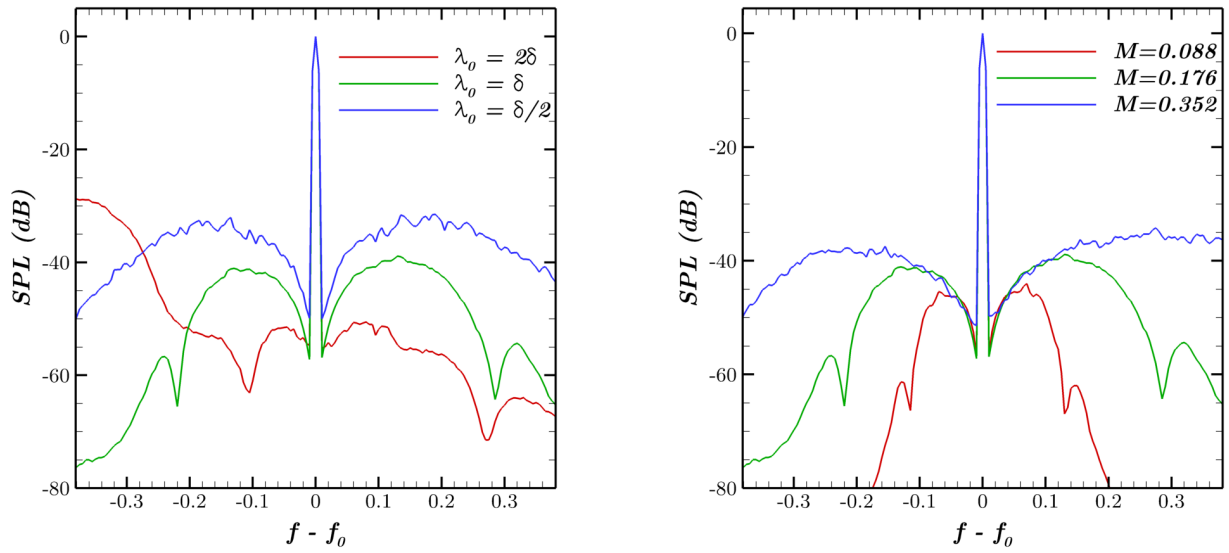

(a) (b)

Figure 4: Comparison between the SPL (a) at $\theta = 90°$ for different source frequencies ($M = 0.176$), (b) at $\theta = 90°$ for different flow velocities ($\lambda_0 = \delta$).

5. Conclusion

The scattering of an harmonic monopole by a turbulent layer with constant width and convected by a uniform flow has been studied numerically. The computational method used is based on solving the linearized Euler equations in the time domain and using a stochastic method to synthesize turbulent fluctuations by filtering a white noise. The different computations realized in this paper focused on the effects of the source frequency and the mean flow velocity. The acoustic spectra deduced from these calculations display sidebands surrounding the incident frequency peak that present similarities with the haystacks observed in previous studies of the spectral broadening by a jet shear layer. These

results are also very similar to the spectra observed for the scattering of an harmonic source by a single convected vortex in previous work. The trends deduced from these computations can also be related to previous results and correlate quite well with the hypothesis that the spectral broadening is linked to a Doppler shift due to the movement of the turbulent eddies acting as sources of the scattered field. This is observed here with the widening of the sidebands when the convection Mach number is increased, and also with the appearance of higher or lower frequency components on the spectra depending on the position of the microphone. Increasing the frequency leads to an important increase of the scattered levels. It is also responsible to changes in the width of the sidebands that have to be related to the incident frequency. Previous work showed that at higher frequency, the scattering by an eddy is more concentrated around the incident wave radiation direction, leading to a smaller relative frequency shift. The consideration of a uniform mean flow allows to used the complete linearized Euler equations without suffering from growing instabilities due to mean flow gradients. Nevertheless, it appears that instabilities are developping when the acoustic waves propagate through the turbulent layer. These instabilities impact the downstream boundary and generate spurious waves that contaminate the acoustic spectra at low frequency. A strategy has to be set up to avoid this phenomenon if calculations have to be done with low frequency sources. In further work the parametric study of the scattering by a turbulent layer will be extended to the parameters of the turbulence generated with the stochastic method. The effects of the layer width, the integral length scale (and the ratio between these two parameters) as well as the turbulent intensity, the correlation time and the spectra (or spatial correlations) of the velocity fluctuations will be considered. Few of these parameters have been considered in the litterature and a numerical study could provide further insight on the mechanisms involved in the scattering by turbulent eddies.

Acknowledgements

This work was partly supported by Rolls-Royce plc through the University Technology Center in Gas Turbine Noise at the University of Southampton and funded by EPSRC Grant EP/K017551/1.

The authors would like to acknowledge the members of the AS/TA department of DLR-Braunschweig for providing the *PIANO* solver and the technical support associated.

The authors also acknowledge the use of the IRIDIS High Performance Computing Facility, and associated support services at the University of Southampton, in the completion of this work.

REFERENCES

1. Brown, E., “Turbulent spectral broadening of backscattered acoustic pulses”, *Journal of the Acoustical Society of America*, **56(5)**, 1974, pp. 1398-1406.

2. Brown, E. & Clifford, S., “Spectral broadening of an acoustic pulse propagating through turbulence”, *Journal of the Acoustical Society of America*, **54(1)**, 1973, pp. 36-39.

3. Brown, E. & Clifford, S., “On the attenuation of sound by turbulence”, *Journal of the Acoustical Society of America*, **60(4)**, 1976, pp. 788-794.

4. Campos, L., “The spectral broadening of sound by turbulent shear layers. Part 1. The transmission of sound through turbulent shear layers”, *Journal of Fluid Mechanics*, **89(4)**, 1978, pp. 723-749.

5. Campos, L., “The spectral broadening of sound by turbulent shear layers. Part 2. The spectral broadening of sound and aircraft noise”, *Journal of Fluid Mechanics*, **89(4)**, 1978, pp. 751-783.

6. Candel, S., Guedel, A. & Julienne, A., “Refraction and scattering of sound in an open wind tunnel flow”, *6th International Congress on Instrumentation in Aerospace Simulation Facilities*, 1975, pp. 288-300.

7. Candel, S., Guedel, A. & Julienne, A., “Radiation, refraction and scattering of acoustic waves in a free shear flow”, *3rd AIAA Aero-Acoustics Conference*, 1976.

8. Clair, V., Gabard, G., "Numerical assessment of the scattering of acoustic waves by turbulent structures", *21st AIAA/CEAS Aeroacoustics Conference*, 2015.

9. Dieste, M., Gabard, G., "Random particle methods applied to broadband fan interaction noise", *Journal of Computational Physics*, **231**, 2012, pp. 8133-8151.

10. Ewert, R., "Broadband slat noise prediction based on CAA and stochastic sound sources from a fast Random Particle-Mesh (RPM) method", *Computers and Fluids*, **37**, 2008, pp. 369-387.

11. Ewert, R., Dierke, J., Siebert, J., Neifeld, A., Appel, C., Siefert, M. & Kornow, O., "CAA broadband noise prediction for aeroacoustic design", *Journal of Sound and Vibration*, **330**, 2011, pp. 4139-4160.

12. Ewert, R., Kornow, O., Delfs, J., Yin, J., Röber, T. & Rose, M., "A CAA based approach to tone haystacking", *15th AIAA/CEAS Aeroacoustics Conference*, n°AIAA-2009-3217, 2009.

13. Ewert, R., Kornow, Tester, B., Powles, C., Delfs, J. & Rose, M., "Spectral broadening of jet engine turbine tones", *14th AIAA/CEAS Aeroacoustics Conference*, n°AIAA-2008-2940, 2008.

14. Ewert, R. & Schröder, W. "On the simulation of trailing edge noise with a hybrid LES/APE method", *Journal of Sound and Vibration*, **270**, 2004, pp. 509-524.

15. Ford, R. & Llewellyn Smith, S., "Scattering of acoustic waves by a vortex", *Journal of Fluid Mechanics*, **386**, 1999, pp. 305-328.

16. Goedecke, G., Wood, R., Auvermann, H., Ostashev, V., Havelock, D. & Ting, C., "Spectral broadening of sound scattered by advecting atmospheric turbulence", *Journal of the Acoustical Society of America*, **109(5)**, 2001, pp. 1923-1934.

17. Howe, M., "Multiple scattering of sound by turbulence and other inhomogeneities", *Journal of Sound and Vibration*, **27(4)**, 1973, pp. 455-476.

18. Kraichnan, R., "The scattering of sound in a turbulent medium", *Journal of the Acoutical Society of America*, **25(6)**, 1953, pp. 1096-1104.

19. Kröber, S., Hellmold, M. & Koop, L., "Experimental Investigation of Spectral Broadening of Sound Waves by Wind Tunnel Shear Layers", *19th AIAA/CEAS Aeroacoustics Conference*, n°AIAA-2013-2255, 2013.

20. Lighthill, M., "On the energy scattered from the interaction of turbulence with sound or shock waves", *Mathematical Proceedings of the Cambridge Philosophical Society*, **49**, 1953, pp. 531-551.

21. McAlpine, A., Powles, C. & Tester, B., "A weak-scattering model for turbine-tone haystacking", *Journal of Sound and Vibration*, **332**, 2013, pp. 3806-3831.

22. Powles, C., Tester, B. & McAlpine, A., "A weak-scattering model for turbine-tone haystacking outside the cone of silence", *International Journal of Aeroacoustics*, **10(1)**, 2011, pp. 17-50.

23. Sijtsma, P., Oerlemans, S., Tibbe, T., Berkefeld, T. & Spehr, C., "Spectral broadening by shear layers of open jet wind tunnels", *20th AIAA/CEAS Aeroacoustics Conference*, n°AIAA-2014-3178, 2014.

24. Tam, C. & Webb, J., "Dispersion-Relation-Preserving finite difference schemes for computational acoustics", *Journal of Computational Physics*, **107(2)**, 1993, pp. 262-281.